

EVOLUTION OF THE WAKE IN A TURBINE BLADE PASSAGE

EDYTA BIJAK-BARTOSIK
WITOLD ELSNER
MARIAN WYSOCKI

*Czestochowa University of Technology, Institute of Thermal Machinery, Czestochowa, Poland
e-mail: welsner@imc.pcz.czyst.pl*

The aim of this paper is an experimental analysis of an unsteady flow field in the blade channel where the unsteadiness was generated by the rotating wheel of cylindrical rods. The measurements were performed with the use of hot-wire technique and double X -wire probe. The application of phase averaging allowed one to reproduce wake motion, which was possible through determination of velocity and turbulence intensity distributions. The role of different mechanisms of wake deformation is discussed. It was also shown that the production of turbulent kinetic energy occurs when the principal stresses within the wake interact with the mean strain.

Key words: rotor-stator interaction, blade passage, wake convection, turbomachinery

1. Introduction

The flow field in turbomachinery is essentially three-dimensional and unsteady. Three-dimensional phenomena like passage vortices, radial flows and end-wall effects play a vital role in the flow, but the most important, especially in the case of long blades, are two-dimensional flow structures which result from rotor-stator interactions. These complex phenomena consist of two separate effects, namely the viscous and potential interactions. The potential interaction reveals itself as flow periodicity induced by moving rotor blades, which would exist even if the fluid was an inviscid one. This effect can cause unsteadiness in both the upstream and downstream direction and its influence decays rapidly with the increase of the axial gap. The viscous interaction is caused by stator

and rotor wakes that produce the circumferential nonuniformity of the flow-field in the axial gap, which are then cut by the rotor blades in the consecutive stage. The viscous wake interaction is only possible downstream of the wake-generating blade row and is much more durable than the potential one and may be advected several chords downstream. Each wake initially represents a perturbation of a uniform flow which is transported with the main flow and subsequently cut into segments by the downstream blade row. Within the blade passage, the wake segments interact with boundary layers and periodically force the laminar-turbulent transition.

A number of research studies have described the kinematics governing convection of the wake through a blade passage. One of the first studies was the work by Meyer (1958), who used potential flow solutions to model wake convection as a perturbation jet through blade cascade. His simplified model, known as the "negative jet", describes the interaction of moving wakes with a blade surface. The concept of Meyer was next developed by Kerrebrock and Mikolajczak (1970), who demonstrated that in the compressor the fluid was taken away from the suction side and transported to the pressure side of the blade profile. Similar observation was done by Binder *et al.* (1984) in an experiment on one-stage air turbine, however in that case the fluid was transported in the opposite direction. Pictures of the flow structure presented in their paper exhibited a visible evolution of stator wakes in the rotor passage, and particularly revealed overturning and underturning regions of the flow, which resulted in, relative to the mean flow, counter rotating vortices. Some numerical studies (Dawes, 1992; Korakianitis, 1991) show that in order to describe the wake behaviour in the blade passage the kinematic assumption is sufficient. Also in most of the research on the wake-induced boundary layer transition (Addison and Hodson, 1990; Schobeiri and Pappu, 1997), the "negative jet effect" was not taken into account.

The recent paper of Stieger and Hodson (2005) has shown however that the transition phenomena on highly loaded turbine blades with high levels of diffusion could be dependant not only on the kinematics of the wake, but also on the "negative jet", which deforms the shear layer. One should also remember that the wake is characterised by a high turbulence intensity, which in the case of turbomachinery could reach the value of 12-13% and considerably exceed the turbulence level outside the wake. Due to the strong spatial gradient of Tu across the wake, it is a natural tendency for the wake to spread in the direction of free stream due to turbulent diffusion. The role of this mechanism was pointed out based on the paper by Hodson and Dawes (1998) who stated that mixing in a blade channel doubles in the presence of wakes. These obser-

rvations were confirmed by Ames and Plesniak (1997) who showed that with the increase of the turbulence level of the free stream the wake spread and dissipated faster, which was a result of amplification of the mixing process by external eddies at the edge of the wake.

It means that the wake passing through the blade row is significantly distorted and, as far as wake deformation is concerned, one can indicate three mechanisms which could be responsible for this effect, that is: convection, "jet effect" and turbulent diffusion.

This paper presents experimental investigation on the wake convection through a turbine blade cascade. A high spatial resolution of measuring points allowed for accurate representation not only of the mean flow quantities but also of fluctuating components. The additionally performed analysis of selected terms of turbulent kinetic energy transport equation allowed to formulate an answer to the above question.

2. Experimental details

The experimental facility (see Zarzycki and Elsner, 2005) consists of an open-circuit wind tunnel equipped with the disturbance (wake) generator and the linear blade cascade. As the periodic wake generator, a wheel of pitch diameter $D_p = 1950$ mm with cylindrical bars rotating in a plane perpendicular to the flow direction is used. The wheel of pitch diameter $D_p = 1950$ mm is equipped with bars of diameter $d = 4$ mm spaced by 204 mm at pitch. The bar diameter was chosen to match the loss of a representative turbine blade profile (Zarzycki and Elsner, 2005). In the present configuration, the rotor-stator axial gap has been set to 72 mm, which corresponds to 34% of the stator axial chord which is often encountered in a real turbine stage. The location of moving cylindrical bars and stator profiles as well as the position of measuring planes are shown in Fig. 1.

The test section of the linear blade cascade consists of five blades, and the measurements are performed on the middle one. The blade profile N3-60 applied in the research is an industrial one, which was used as a stator vane of the high-pressure part of the TK-200 turbine produced the Polish manufacturer (formerly ZAMECH, now ALSTOM). The main geometrical parameters of the cascade are: blade chord length $b_s = 300$ mm, pitch $t_s = 240$ mm, and blade stagger angle $\alpha_s = 43^\circ 35'$. The Reynolds number, based on the chord and exit conditions, is $6.0 \cdot 10^5$ and the inlet freestream turbulence equals $Tu = 3.8\%$. Taking into account the velocity of moving bars as well as the

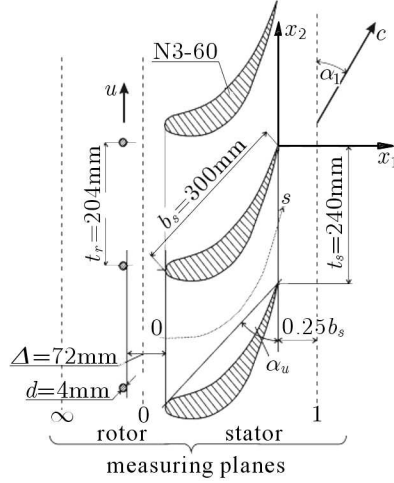


Fig. 1. Scheme of the tested section

spacing of the bars, the frequency of incoming wakes is equal $f_d = 59\text{ Hz}$, which corresponds to the reduced frequency $St = 1.22$. The St parameter is defined as $St = f_d b_s / C_0$, where C_0 is the velocity at the inlet to the blade cascade.

The measuring area (see Fig. 2) covers the regions between the wake generator and the blade cascade, the blade passage as well as the region behind the cascade. It consists of 850 points evenly (with 10 mm distance) distributed in the axial and circumferential directions. Such a dense mesh allows for accurate representation not only of the mean flow quantities but also of fluctuating components.

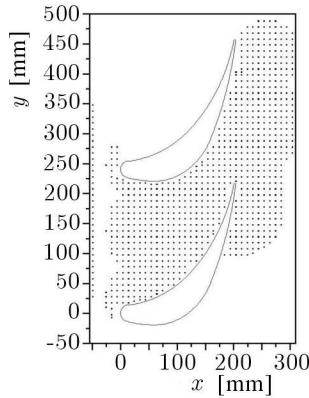


Fig. 2. Blade channel area covered by measurement points

Experimental investigations of the velocity field in the channel have been performed using a double wire probe combined with the DISA 55M System hot-wire anemometer coupled to a PC computer. The computer was equipped with a 12-bit analog-digital (A/D) converter with the input range 0-12 V. The hot-wire was calibrated in-situ before and after the experiment. To have the possibility of the phase locked analysis, the reference signal was additionally measured. The velocity signals were recorded for 20s with the frequency 25 kHz. Considering the velocity range covered during the experiment, the uncertainty analysis of recorded hot-wire signals revealed the mean measuring error on the level $\sim 3\%$. This value included both the uncertainty of the experimental equipment applied and the measuring technique.

3. Wake convention in the blade passage

The tested blade cascade is an accelerating one with the acceleration factor about 3.2, where this coefficient concerns the change of time-mean velocity along the center line of the channel. However, one should remember that the level of mean velocity changes also in the crosswise direction of the channel. The spatial distribution of the mean velocity in the blade passage is presented in Fig. 3a. A higher level of velocity near the suction side of the upper blade and a clearly lower close to the pressure surface of the bottom blade are observed. Particularly distinct difference of the velocity is visible in the first part of the channel in the range of the axial coordinate $x = 20-160$ mm. However, the area of maximum velocity appears near the exit of cascade, in the region of minimum pressure at the suction side. The strong acceleration is due to the decrease of cross-sectional area of the channel. The deformation of the flow field is additionally caused by the curvature of the blade profile. Moreover, the visible velocity defect is seen behind the lower blade.

The unsteady flow in the blade channel can be visualized by the perturbation velocity, which is defined as the difference between ensemble average velocity and the time average velocity according to

$$\langle \tilde{c}_1 \rangle = \langle C_1 \rangle - \bar{C}_1 \quad \langle \tilde{c}_2 \rangle = \langle C_2 \rangle - \bar{C}_2 \quad (3.1)$$

where $\langle C_1 \rangle$ and $\langle C_2 \rangle$ are the ensemble averaged velocity components.

The perturbation velocity vectors superimposed on the turbulence intensity $\langle Tu \rangle$ distributions presented at four time instants (Fig. 4) provide a clear picture of the wake location. Figure 4a shows the moment when the wake is

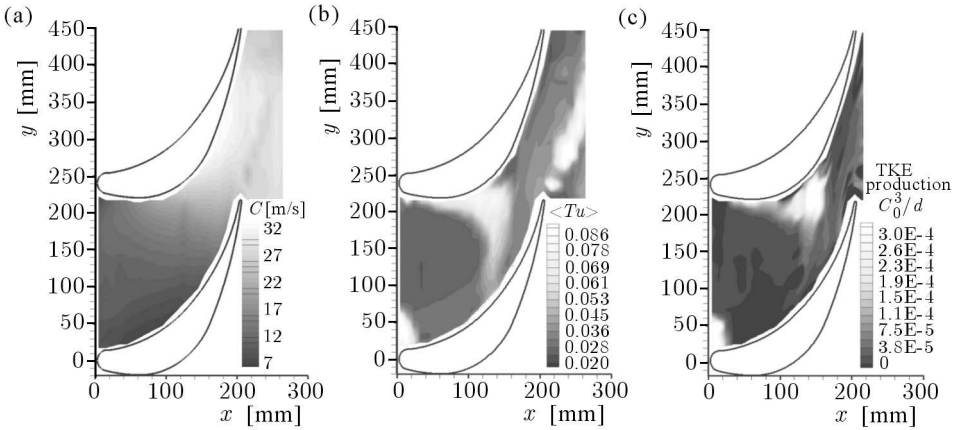


Fig. 3. Mean velocity distribution (a), turbulence intensity for time instant $\tau/T = 0.2$ (b), TKE production for time instant $\tau/T = 0.2$ (c)

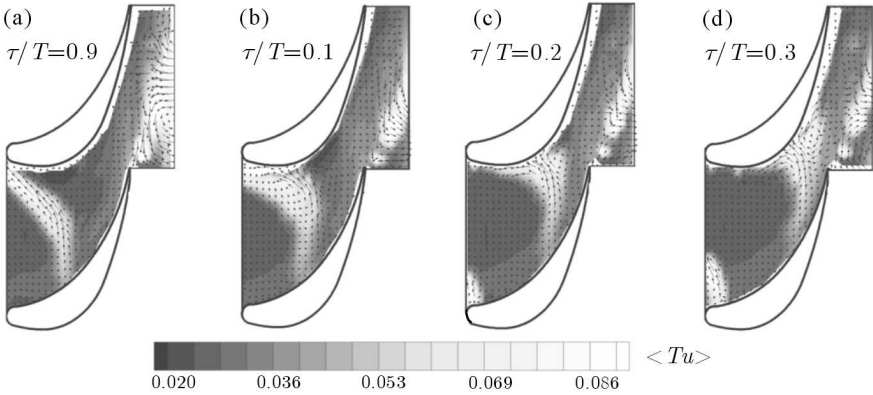


Fig. 4. Distribution of turbulent intensity for four time instants with superimposed vectors of perturbation velocity

approaching the leading edge of the upper blade. One may notice the beginning of deformation of the wake nearby the pressure surface of the lower blade caused by lower convection velocity in this region. The vectors in the wake indicate the existence of the "jet effect" pointing towards the source of the wake and show relative transport of the fluid from the pressure side of the blade. In the next moment of time (Fig. 4b), the wake located in the central part of the picture is bowed and stretched due to strong acceleration close to the suction side of the blade. Then the wake moves towards the exit of the cascade (Fig. 4d) where two counter rotating vortices (visible only in the relative frame), resulting from the "jet effect", are also seen. The perturbation from the "negative jet" accelerates the flow downstream and decelerate upstream

of the wake centre. The counter rotating vortices cause strong stretching of the wake in the vicinity of the suction surface of the blade, both in the upstream and downstream direction. From the mass conservation law, it results that the mass displaced toward the suction surface has to be carried away back to the pressure side of the blade again. These vortices were convected downstream and acted as an additional source of unsteadiness of the main flow and boundary layers on the blades surfaces. It should be noted however, that these vortices could only be identified by subtracting the mean value from the overall velocity.

Looking at Fig. 4c,d, one could observe the stretching of the wake in the near wall region of the pressure side of the blade and the resulting sliding of the low wake "leg" along the wall. Similar observations were reported by Kost *et al.* (2000). Additionally, the decrease of the wake width in this region is seen. This phenomenon, however, has no significant influence on the boundary layer and on the generation of losses. One may also observe that the intensity of the wake decays as it is moving in the streamwise direction along the pressure side of the blade. On the other hand, the increase of Tu close to the suction side in the central part and at the exit of the channel is seen.

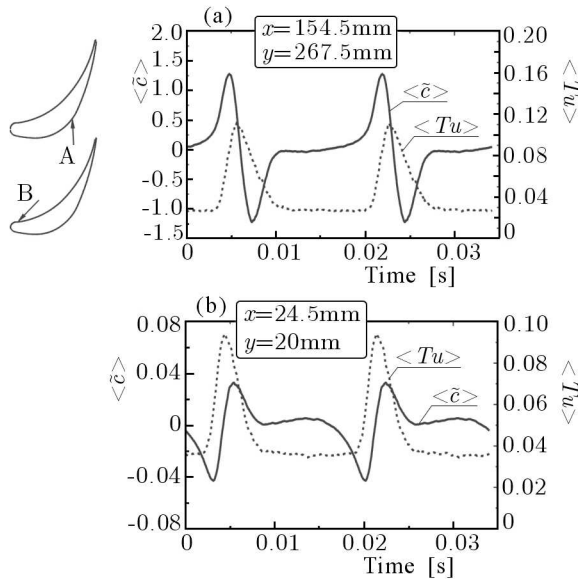


Fig. 5. Time traces of perturbation velocity and turbulence intensity in the vicinity of the suction (A) and pressure side (B)

Figure 5 presents time traces of the above parameters recorded at two chosen points, one located close to the suction side of the blade and the other close

to the pressure side of the blade. For the first point (Fig. 5a), the characteristic increase of velocity in the front of the wake, which is due to the "jet effect", is seen. It is accompanied with a high level of Tu of an order of 11%. Close to the pressure side, the turbulence intensity in the wake center drops from 9.5% (Fig. 5b) to only about 3.5%. The traces of the perturbation velocity confirm conclusions of the different character of the flow near the pressure side than observed close to the suction surface. The fluid accelerates more in the back of the wake than in its front part, which is again a consequence of the "jet effect".

The above analysis confirms that the change of the shape and width of the wake, especially at the edges of the blade channel is also due to the "jet effect". The "jet effect" causes the appearance of counter rotating vortices, in the relative frame of references seen on the perturbation velocity distributions. These vortices not only perturb the flow but also act as an additional source of unsteadiness of the boundary layer on the blade surface.

4. Analysis of chosen terms of TKE transport equation

A more detailed analysis of the process proceeding within the wake is possible by the determination of chosen terms of the turbulent kinetic energy transport equation. It was decided to take into account: production of turbulent kinetic energy and turbulent diffusion.

For the considered two-dimensional flow, turbulent kinetic energy (denoted as TKE) is determined according to the following equation

$$\langle q'^2 \rangle = \frac{1}{2}(\langle c_1'^2 \rangle + \langle c_2'^2 \rangle) \quad (4.1)$$

where c_1' and c_2' are two fluctuating components of the velocity. Based on that the ensemble averaged turbulence intensity component is calculated

$$\langle Tu \rangle = \frac{\langle \sqrt{q'^2} \rangle}{C_0} \quad (4.2)$$

The flux of energy which increases the kinetic energy of the fluid at the expense of the mean flow is the production. The ensemble averaged production of TKE in the blade channel is obtained, taking into account the ensemble averaged Reynolds stresses and ensemble average spatial velocity derivatives, i.e.

$$-\langle c_1' c_1' \rangle \frac{\partial \langle C_1 \rangle}{\partial x} - \langle c_2' c_2' \rangle \frac{\partial \langle C_2 \rangle}{\partial y} - \langle c_1' c_2' \rangle \left(\frac{\partial \langle C_1 \rangle}{\partial x} + \frac{\partial \langle C_2 \rangle}{\partial y} \right) \quad (4.3)$$

Neglecting the dissipation term, which is difficult to estimate, only the diffusion effect is worth considering. The turbulent diffusion is the diminishing flux of the whole energy budget, and for the case considered it is determined as

$$\left\langle c'_1 \frac{\partial q'^2}{\partial x} \right\rangle + \left\langle c'_2 \frac{\partial q'^2}{\partial y} \right\rangle \quad (4.4)$$

Figure 3 shows three pictures: mean velocity distribution (a), turbulent intensity (b) and production of TKE (c) for the time instant $\tau/T = 0.2$. The last quantity was reduced by the ratio C_0^3/d . One can easily notice the increased value of turbulent intensity in the wake region at the rear part of the blade channel, where a high velocity gradient is present. At the same time, the rise of production is observed at the same location. It confirms the observation already made by Stieger and Hodson (2005) for a highly loaded LP turbine blade, who stated that the elevated level of turbulence could be due to increased production of TKE. Because the production variation is inherently connected with the wake position, one can deduce that the turbulence is generated also in the shear layers of the wake where turbulent stresses are present.

Further analysis concerns the role of turbulent diffusion in the wake deformation process. The analysis was performed for the initial part of the channel indicated in Fig. 6 by the dashed line. Figure 6 presents data obtained for the three time instants ($\tau/T = 0.95, 0.05, 0.15$) where the upper graphs show the turbulence intensity distribution with superimposed perturbation velocity vectors that reveal the wake location. The middle graphs present TKE production and the bottom one turbulent diffusion calculated according to equations (4.3) and (4.4), respectively. The turbulent diffusion was reduced by the ratio C_0^3/d .

It is seen that once the wake enters the blade channel, the two regions of increased turbulence appear, one close to the blade edge and the other placed far away from the blade. In this first region, the turbulent kinetic energy is generated due to the interaction of the wake with the leading edge of the blade and, as it may be seen for further time instants, its elevated region disappears. The second region is developing as the wake moves downstream. For $\tau/T = 0.05$, the wake is being deformed and shifted towards the blade surface by the mean flow. At the same time, due to straining forces, the increased production of TKE in this region appears. Further downstream ($\tau/T = 0.15$) the wake is strongly bent and pushed towards the blade surface, and the production of TKE is enhanced. Further, up to $\tau/T = 0.40$ (what is not shown here), the wake passes through the strongest velocity gradient, where the inten-

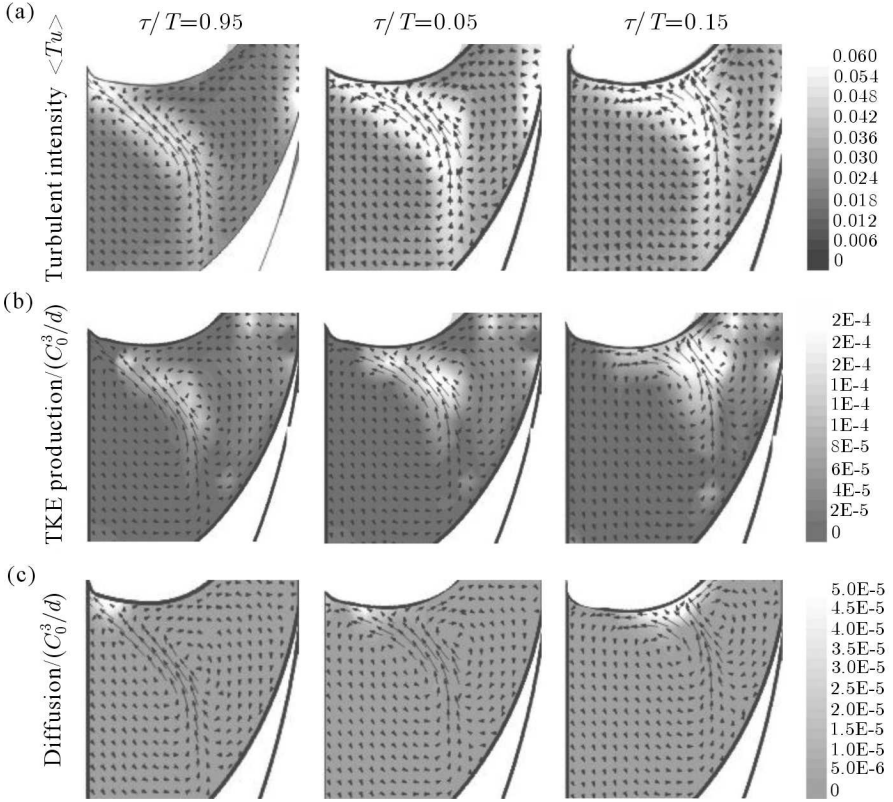


Fig. 6. Channel inlet area: turbulence intensity distribution (a), TKE production (b), diffusion (c), with superimposed vectors of perturbation velocity

se growth of TKE is accompanied by the increase of TKE production. Looking at the location of high production spot (white area), one can conclude that the TKE production proceeds in the front part of the wake and it leads to the growth of TKE. It means that high turbulent stresses present within the wake interact with the mean velocity gradient and it results in an increase of TKE production. These observations confirm the conclusion formulated above concerning the significant role of energy production in the increase of TKE. Taking into account the turbulent diffusion, its value is very low in the entire blade channel. A noticeable value of diffusion is only observed (see Fig. 6, $\tau/T = 0.15$) close to the suction side of the profile, where a high level of TKE is present. However, its value is still very low in comparison with the production (below 1%).

Comparing particular terms of the energy equation, it is necessary to say that generation of additional turbulent energy is only due to the production,

while dissipation is only responsible for the extraction or addition of energy to the particular region of the flow. It is also necessary to say that the analysis performed based on the results presented in Fig. 6 does not indicate the direction of energy fluxes. It only allows one to show where, relative to the wake position, the increase value of production or diffusion is present.

5. Conclusions

The analysis presented above proves that the convection is the main mechanism responsible for the wake deformation and that the role and share of turbulent diffusion is of minor importance. Only a slight increase of diffusion is observed in the rear part of the blade channel, where TKE production appears. The elevated production of kinetic energy in the wake passing through the region of high spatial velocity gradient causes an increased level of turbulence. The production of TKE is strongest in the region where the Reynolds stresses and the strain rate field of the main flow are aligned. That is why it mainly occurs in the front part of the wake and leads to the growth of TKE.

The change of shape and width of the wake, especially at the edges of the channel is evidently caused by the "jet effect". The "jet effect" causes the appearance of counter-rotating vortices on both sides of the wake, seen on the perturbation velocity distributions. These vortices not only perturb the flow but also act as an additional source of unsteadiness of the boundary layer on the blade surface.

Acknowledgements

The research was supported by the Polish State Committee for Scientific Research under the statutory funds BS-01-103-301/2004/P and partly within the research project UTAT – "Unsteady Transitional Flows in Axial Turbomachines", funded by the European Commission under contract number GRD1-2001-40192.

References

1. ADDISON J.S., HODSON H., 1990, Unsteady transition in an axial-flow turbine: Part 2 – Cascade measurements and modeling, *ASME Journal of Turbomachinery*, **112**, 215-221
2. AMES F.E., PLESNIAK M.W., 1997, The influence of large-scale, high-intensity turbulence on vane aerodynamic losses, wake growth, and the exit turbulence parameters, *Journal of Turbomachinery*, **119**, 182-192

3. BINDER A., FORSTER W., KRUSE H., ROGGE H., 1984, An experimental investigation into the effect of wakes on the unsteady turbine rotor flow, *ASME Journal of Engineering for Gas Turbines and Power*, **107**, 1039-1046
4. DAWES B., 1992, The simulation of three dimensional viscous flow in turbomachinery geometries using a solution-adaptive unstructured mesh methodology, *ASME Journal of Turbomachinery*, **114**, 528-537
5. HODSON H.P., DAWES W.N., 1998, On the interpretation of measured profile losses in unsteady wake-turbine blade interaction studies, *ASME J. of Turbomachinery*, **120**, 276-284
6. KERREBROCK J.L., MIKOLAJCZAK A.A., 1970, Intra-stator transport of rotor wakes and its effect on Compressor Performance, *ASME Journal of Engineering for Power*, **92**, 359-368
7. KORAKIANTITIS T., 1991, On the propagation of viscous wakes and potential flow in axial-turbine cascades, *ASME Paper No. 91-GT-373*
8. KOST F., HUMMEL F., TIEDEMANN M., 2000, Investigation of the unsteady rotor flow field in a single HP turbine stage, *ASME 2000-GT-432*
9. MEYER R.X., 1958, The effects of wakes on the transient pressure and velocity distributions in turbomachines, *Trans. Journal of Basic Engineering*, **80**, 1544-1552
10. SCHOBEIRI M.T., PAPPU K., 1997, Experimental study on the effect of unsteadiness on boundary layer development on a linear turbine cascade, *Exp. in Fluids*, **23**, 306-316
11. STIEGER R.D., HODSON H.P., 2005, The unsteady development of a turbulent wake through a downstream low pressure turbine blade passage, *ASME Journal of Turbomachinery*, **127**, 388-394
12. ZARZYCKI R., ELSNER W., 2005, The effect of wake parameters on the transitional boundary layer on turbine blade, *Proc. IMechE*, **219**, Part A, *Journal of Power and Energy*, 471-480

Ewolucja śladu spływowego w międzyłopatkowym kanale turbinowym

Streszczenie

W pracy przedstawiono wyniki eksperymentalnej analizy niestacjonarnego przepływu przez kanał łopatkowy turbiny, dla którego to przypadku zaburzenia generowane były na wlocie do kanału przez wirujący wieniec prętów cylindrycznych. Pomiarzy zostały przeprowadzone przy wykorzystaniu dwuwłókowej sondy termooanometrycznej typu *X* dla gęstej siatki pomiarowej. Zastosowanie metody uśredniania fazowego pozwoliło na odtworzenie ruchu śladu i analizę jego deformacji w przepływie

przez palisadę w kolejnych chwilach czasu. W artykule podjęto dyskusję roli różnych mechanizmów odpowiedzialnych za deformację śladu, wskazując na dominującą rolę konwekcji. Wykazano, że za wzrost energii kinetycznej turbulencji w śladzie odpowiedzialna jest produkcja energii kinetycznej turbulencji będąca efektem oddziaływania naprężeń turbulentnych w śladzie z silnym gradientem prędkości w kanale międzyłopatkowym.

Manuscript received May 26, 2008; accepted for print October 24, 2008